The Journal of Experimental Biology 212, 78-88
Published by The Company of Biologists 2009
doi:10.1242/jeb.024612

Multiplicity of expression of Na^+,K^+–ATPase α-subunit isoforms in the gill of Atlantic salmon (*Salmo salar*): cellular localisation and absolute quantification in response to salinity change

Steffen S. Madsen*, Pia Kiilerich and Christian K. Tipsmark
Institute of Biology, University of Southern Denmark, 5230 Odense M, Denmark
*Author for correspondence (e-mail: steffen@biology.sdu.dk)

Accepted 29 October 2008

SUMMARY

The ability to reverse the net direction of gill ion transport in response to a salinity change is critical for euryhaline teleosts and involves a complex cellular and molecular remodelling of the gill epithelium. The present study aimed to clarify the cellular localisation and exact quantitative inter-relationship of Na^+,K^+–ATPase α- and β-subunit transcripts in Atlantic salmon gill during salinity change. The combined expression level of all α-isoforms in the gill increased by 100% after freshwater (FW) to seawater (SW) transfer. The α_{1a} and α_{1b} isoforms were both in the range 1–6 amol 20 ng^{-1} total RNA; α_{1a} decreased and α_{1b} increased after SW-transfer, their ratio changing from 5:1 in FW to 0.26:1 in SW. The α_{1c} and α_3 levels were 10- and 100-fold lower, respectively. The β_1-subunit mRNA level was 0.1–0.3 amol 20 ng^{-1} total RNA, thus much lower than the sum of α-subunits. Even though increasing 3-fold after SW-transfer, β-subunit availability may still limit functional pump synthesis. The mRNAs of the predominant α_{1a} and α_{1b} isoforms were localised by *in situ* hybridisation in specific gill cells of both FW and SW salmon. Labelling occurred mainly in presumed chloride cells and cells deep in the filament but occasionally also on lamellae. Overall, the salinity-induced variation in labelling pattern and intensity matched the quantification data. In conclusion, the predominant switching of Na^+,K^+–ATPase α-subunit isoform mRNA during salinity acclimation reflects a marked remodelling of mitochondrion-rich cells (MRCs) in the gill and probably tuning of the pump performance to accomplish a net reversal of gill ion transport in hypo- and hypertonic environments.

Key words: absolute quantification, chloride cell, *in situ* hybridisation, mRNA.

INTRODUCTION

The branchial mechanisms and cellular targets responsible for ion-regulatory homeostasis in teleosts have been subject to extensive research since the pioneering investigations of Homer-Smith, Krogh and Keys in the early 20th century (Evans, 2008). Nonetheless, important issues still need to be clarified regarding the molecular details of ion transport. Among the various cell-types in the gill, the mitochondrion-rich so-called chloride cells (MRCs) in conjunction with their neighbouring cells (accessory- and pavement cells) are of principal importance in ion-uptake and ion-excretion. Chloride-secreting cells were first discovered and named by Keys and Wilmer (Keys and Wilmer, 1932), and were assigned an important role in salt secretion in a number of marine teleosts. Subsequently, MRCs have been identified by different techniques based on their ultrastructural and biochemical properties (for reviews, see Evans et al., 2005; Hwang and Lee, 2007). One common way of visualising MRCs exploits the dense abundance of the Na^+,K^+–ATPase enzyme in the basolateral membrane networks of these cells. Thus, immunostaining with generic anti-Na^+,K^+–ATPase antibodies is a common procedure to identify these cells. MRCs have been classified into several subtypes, based on ultrastructure (α- and β-type), localisation within the gill (in lamellae, at base of lamellae, interlamellar in filament, etc.), dynamics in response to salinity change (recruitment to/from lamellae, hyperplasia in filament) or expression of additional ion-transport proteins (V-type H^+–ATPase, Cl^-/HCO_3^- exchanger, CFTR-chloride channel, Na^+,K^+2Cl^- cotransporter) (for reviews, see Evans et al., 2005; Hwang and Lee, 2007). There is consensus that in euryhaline teleost species, ion transporting cells may appear in both filament and lamellar positions, in some cases depending on salinity and other stressors, and also with clear species specific differences (Tipsmark et al., 2007; Uchida et al., 1996; Varsamos et al., 2002). At least in salmonids, it has been convincingly demonstrated that ionocytes appear in both locations in freshwater (FW) whereas in seawater (SW) most lamellar MRCs regress and the filament MRCs increase in number and particularly in size (Seidelin et al., 2000; Uchida et al., 1996). This led these authors to propose that lamellar cells are involved in ion-uptake (FW–MRC) and filament cells may have a dual function in both ion-secretion (SW–MRC) and ion-uptake.

The active and passive steps in gill ion-translocation have been unravelled from studies involving both stenohaline and euryhaline teleosts of FW as well as SW origin. At both salinities, net ion-transfer is based on the activity of Na^+,K^+–ATPase as the primary energy-consuming step, even though in certain species this may be supplemented by the active transfer of protons by V-type H^+–ATPase (Evans et al., 2005). The level of complexity has recently increased by the discovery of three different isoforms of the α_1-subunit in gill tissue of *Oncorhynchus mykiss* (Richards et al., 2003): α_{1a}, α_{1b} and α_{1c}. These are present in addition to an α_3 isoform, which has also been described in a number of other species [*Oreochromus mossambicus* (Lee et al., 1998); *Danio rerio* (Rajarao et al., 2001); *Trematomus spp* (Guynn et al., 2002)]. The relative abundances of some of these isoforms in whole-gill RNA extracts have been investigated during salinity acclimation in a few studies

[*O. mykiss*, *Salvelinus alpinus*, *Salmo salar* (Richards et al., 2003; Bystrianski et al., 2006; Bystrianski et al., 2007); *O. nerka* (Shrimpton et al., 2005); *Fundulus heteroclitus* (Scott et al., 2004)]. Based on analyses of relative mRNA levels by real-time quantitative polymerase chain reaction (RT-QPCR), the general picture emerging from these studies is that salinity induces a reciprocal regulation (switching) – primarily of the α_{1a} and α_{1b} isoforms, α_{1a} generally being upregulated in FW and α_{1b} being upregulated in SW. This led Richards et al. to suggest that the α_{1a} is a FW-isoform driving in ion-uptake whereas α_{1b} is a SW-isoform driving ion-secretion (Richards et al., 2003). Accordingly, the α_{1b} is upregulated during salmon smoltification in FW – a process preparing the juvenile fish for movement into the marine environment (Nilsen et al., 2007). In support of this, Jorgensen recently showed that a few particular amino acid differences between the two isoforms may critically influence cation binding properties, and reduce the Na^+:ATP ratio from 3:1 in α_{1b} to 2:1 in the α_{1a} isoform (Jorgensen, 2008). In *O. mykiss* and *S. salar*, the presence of a lysine residue instead of asparagine at site 783 in transmembrane segment 5 of the α_{1a} isoform thus leads to this isoform being energetically better suited for Na^+ transport against extreme electrochemical gradients, as is the case for ion uptake in FW.

Only relative measures of mRNA abundance have been reported so far, and nothing is known neither about the quantitative relationship between the four isoforms nor of their cellular localisation in the gill. Based on relative measures, attempts have been made to calculate changes in the total abundance of α-subunit mRNA during salinity changes (Bystrianski et al., 2006; Bystrianski et al., 2007); however, such an arithmetic exercise requires absolute quantification and is invalid when based on relative measures. The purpose of the present study was to investigate the cellular localisation of the α-subunit isoform mRNAs in the Atlantic salmon gill by *in situ* hybridisation (ISH) and to clarify the time course and the exact quantitative interrelationship of the four α-subunit isoforms in the gill when subject to salinity change. The β_1-subunit, which is needed in a 1:1 ratio with the α_1-subunit for functional maturation and membrane targeting (Scheiner-Bobis, 2002) was also quantified to give insight into the stoichiometric relationships between the two subunits.

MATERIALS AND METHODS

Fish and sampling

One-year old Atlantic salmon (*Salmo salar* L., Ätran strain obtained from Danish Center for Wild Salmon, Randers, Denmark) were kept in outdoor tanks with flowing Odense city tap water (in mmol l^{-1}: 1.4 Cl^-, 1.5 SO_4^{2-}, 1.5 Na^+, 0.16 K^+, 3 Ca^{2+}, 0.6 Mg^{2+}; 5.5 total CO_2 content; pH 8.3) at environmental temperatures and exposed to natural daylight through smoltification. After smoltification in August 2006, these fish were transferred to indoor conditions in 500-l fibre-glass tanks at 14°C at 12 h:12 h light:dark cycle and were considered to be post-smolts. In October 2006, subgroups were either transferred to 28 p.p.t. artificial, aerated, re-circulated and filtered SW (Red Sea Salt, Eliat, Israel) or sham transferred to FW. Eight fish from each salinity were sampled 12 h, 24 h, 3 days and 7 days after transfer together with eight fish at 0 h as a control group. Fish were stunned with a blow to the head and blood collected from the caudal vessel. After cutting the spinal chord and pithing of the brain, a second gill arch was immediately dry frozen in liquid nitrogen for RNA purification and the other second gill arch was frozen in sucrose–EDTA–imidazol buffer (SEI: 300 mmol l^{-1} sucrose, 5 mmol l^{-1} Na_2EDTA, 50 mmol l^{-1} imidazol, pH 7.3) for analysis of Na^+,K^+–ATPase enzymatic activity (McCormick, 1993). Experimental protocols were approved by the Danish Animal Experiments Inspectorate being in accordance with the European convention for the protection of vertebrate animals used for experiments and other scientific purposes (#86/609/EØF).

Real-time QPCR analysis

Total RNA was purified using GenElute™ Mammalian Total RNA kit (Sigma Chemical Co., St Louis, MO, USA) according to the manufacturer's recommendations. RNA concentration and purity was determined by measuring A260/A280 on undiluted samples on a Nanodrop spectrophotometer (Nanodrop Technologies, Wilmington, DE, USA). One µg RNA was DNase treated (Promega, Madison, WI, USA) and then reverse transcribed using 2 µg oligo dT primers (GE Healthcare Bio-Sciences, Little Chalfont, UK) and 200 units MMLV reverse transcriptase (Invitrogen, Carlsbad, CA, USA) for 1 h at 37°C in the presence of 40 units of RNAguard (GE Healthcare) in a total volume of 25 µl. At the end the cDNA was diluted to 50 µl with milliQ H_2O. Real-time PCR analysis using SYBR Green detection was performed on a Mx3000-P PCR machine (Stratagene, La Jolla, CA, USA) using standard software settings including adaptive baseline for background detection, moving average and amplification based threshold settings with the built-in FAM (5-carboxyfluorescein) filter (excitation wavelength, 492 nm; emission wavelength, 516 nm). Reactions were carried out with 1 µl cDNA, 150 nmol l^{-1} forward and reverse primer (Table 1) and 1× SYBR® Green JumpStart™ Taq ReadyMix™ (Sigma Chemical Co.) in a total volume of 25 µl. Cycling conditions were: 95°C for 120 s followed by 40 cycles of 95°C for 30 s and 60°C for 60 s. Melting curve analysis was performed following each reaction to confirm the presence of only a single product in the reaction.

Table 1. Sequences of synthetic polynucleotides used as templates for generation of standard curves, primers and GenBank references used for mRNA quantification of α_{1a}, α_{1b}, α_{1c}, α_3 and β_1 subunit isoforms of the *Salmo salar* Na^+,K^+–ATPase

Transcript	cDNA sequence (5′-3′) used for quantification*	Primers 5′-3′	Reference
α_{1a}	TTCCAAAGGCAAATGGGTTTAATATCATTGTAAAAATGAACGATTCATTACAA	F: CCCAGGATCACTCAATGTCAC	*O. mykiss*/
	GGCAATACTGCAGCAGAGTGACATTGAGTGATCCTGGGACGGCCTC	R: CCAAAGGCAAATGGGTTTAAT	AY319391
α_{1b}	GCAGCTGAGTGCACCATCACAGTGTTCATTGGATGTAATGATAAGGTAGCAT	F: CTGCTACATCTCAACCAACAACATT	*O. mykiss*/
	ATTGAAATGTAGTGTAATGTTGTTGGTTGAGATGTAGCAGCAGAGTG	R: CACCATCACAGTGTTCATTGGAT	AY319390
α_{1c}	CAGAACTTAAAATTCCGAGCAGCAAGACAACCATGCAAGAACTTGAGCGATG	F: GAGAGGGAGACGTACTACTAGAAAGCA	*O. mykiss*/
	CAAACGGGATGCTTTCTAGTAGTACGTCTCCCTCTCCACCCAACCTC	R: CAGCAAGACAACCATGCAAGA	AY319389
α_3	CTTGTGGGTATCAGGCTCAACTGGGACGACCGCGCTTGCAACGACCTGGA	F: TCCACGATCTTCCTCTGTTCA	*S. salar*/
	AGACAGCTATGGCCAGCAATGGACATATGAACAGAGGAAGATCGTGGAG	R: TTGTGGGTATCAGGCTCAACT	CX355357
β_1	TTACCGGCGTCCTCCTCTCTCTTGTTGGTGCAAAAGATGGGCATGACGTTG	F: CCAATGAAAGCATCCCTAG	*S. salar*/
	GGCTGGACCTTGGTCTGCGCTCCCTCAGGGATGCTTTCATTGGAGCTG	R: GGCGTCCTCCTCTCTCTTGT	AJ250810

The sequence of each synthetic polynucleotides was based on the corresponding reverse strand, anti-sense gene sequence listed as reference. *Shaded areas of the polynucleotide sequences indicate primer regions.

Negative control reactions using DNase treated total RNA from representative samples were used to analyse carry over of genomic DNA. In all samples and with all primers there was negligible genomic contamination.

Primers

The primers used to amplify the Na^+,K^+–ATPase α_{1b}, and α_{1c} isoforms were the same as used by Richards et al. (Richards et al., 2003). These were designed for *O. mykiss* and have been successfully used for *S. salar* by Bystrianski et al. (Bystrianski et al., 2006). The sequences of the primers used for the α_{1a} isoform in *O. mykiss* (Richards et al., 2003) and *S. salar* (Bystrianski et al., 2007) in previous studies were identical to the α_{1b} sequence in the primer region (mismatch 1/18 and 2/18 for forward and reverse primers, respectively) and in our hands, were found not to be specific for the α_{1a} isoform (not shown). Therefore, we designed specific primers for the α_{1a} near the 3′ terminus of the complete mRNA sequence (for *O. mykiss*) in order to obtain maximum isoform specificity. For the α_3 isoform we designed primers based on a *S. salar* EST sequence (acc. no. CX355357), which is 99% identical to the *O. mykiss* α_3 isoform. For the β_1-subunit, primers were designed based on a partial *S. salar* β_1-sequence (acc. no. AJ250810). Primers were designed using the NetPrimer software (Premier Biosoft International, CA, USA) with standard settings and double checked using the Primer3 software (Rozen and Skaletsky, 2000) and BLASTed. All primers were tested for non-specific product amplification and primer–dimer formation using both melting curve analysis and agarose gel verification. All primers were synthesised by DNA Technology A/S (Aarhus, Denmark).

Standard curves and calculations

In order to convert threshold cycle (Ct)-values from a given PCR reaction into absolute quantities of the corresponding transcript, it was necessary to generate a standard curve for each of the five transcripts of interest (α_{1a}, α_{1b}, α_{1c}, α_3 and β_1). Therefore, a specific single stranded polynucleotide (approximately 100 bases long) (Table 1) based on the antisense chain of each α-isoform gene sequence was synthesised (Invitrogen), thus defining the amplicon of each primer pair. The amount of specific polynucleotides used per PCR reaction to generate the standard curves ranged from 0.01 amol to 1 fmol. This generated Ct-values in the range 10–28 depending on the amplicon. For each standard curve, the regression line was then used for calculations of cDNA quantity in the unknown samples. Ct-values of the unknown samples were always within the range of the actual standard curve. Amplification efficiencies of the five PCR reactions were in the range of 92 to 103% both when using polynucleotides or actual cDNAs amplified from tissue RNAs as template.

ISH

In a separate experiment using long term (>3 weeks) FW- and SW-acclimated *S. salar*, blocks of gill tissue (2 mm wide) were quickly removed from euthanised fish. After trimming away the cartilage rod, a 2–3 mm gill block was placed in a small alufoil mould, embedded in Optimal Cutting Temperature Compound (Miles, Eikhart, IN, USA) and quick frozen on dry ice. The specimens were stored desiccated at –80°C until further processing. Sections (8–10 μm) of the frozen specimens were then cut on a cryostat at –14°C, transferred to Superfrost Plus glass slides (Erie Scientific Company, Portsmouth, NH, USA) and dried for 1 h at 50°C. The sections were then transferred to –80°C until further processing. Upon use, the sections were thawed at room temperature, soaked in 96% ethanol for 1 h and dried at 37°C for 30 min. They were incubated overnight under cover glass with 3 pmol ml^{-1} of alkaline phosphatase (AP) labelled cDNA probes (Table 2) in hybridisation buffer at 37°C in a sealed chamber with 100% humidity. Depending on the base composition and theoretical melting point of the DNA–RNA duplexes (T_m) hybridisation conditions were varied (see Table 2): 30–50% formamide, 1.5–4× saline sodium citrate buffer (SSC: 165 mmol l^{-1} NaCl, 3.3 mmol l^{-1} sodium citrate), 1× Denhardt's solution (0.2 mg ml^{-1} Ficoll, 0.2 mg ml^{-1} polyvinyl pyrrolidon, 0.2 mg ml^{-1} bovine serum albumin), 10% dextran sulphate, 10 μg ml^{-1} single-stranded salmon sperm DNA. The hybridisation temperature was always 37°C, which is 20–25°C lower than the theoretical T_m of all probes in solution and thus near the optimal temperature for hybridisation in the tissue (Augood et al., 1993; Tecott et al., 1987). After incubation, the cover glass was carefully removed and the sections rinsed in three 30 min changes of 3× SSC (22.5 mmol l^{-1} NaCl, 2.3 mmol l^{-1} sodium citrate, pH 8.0) at 37°C followed by two 10 min rinses in post-hybridisation buffer (0.01 mol Tris-HCl, 0.15 mol NaCl, pH 9.5) at room temperature. For colour development, the specimens were incubated in freshly made AP developer buffer (0.32 mg ml^{-1} nitro blue tetrazolium (NBT; Sigma Chemical Co.), 0.17 mg ml^{-1} 5-bromo-4-chloro-3-indolyl phosphate (BCIP; Sigma Chemical Co.), 0.1 mol Tris-HCl, 0.1 mol NaCl and 0.05 mol $MgCl_2$, pH 9.5) for 1 to 3 days in the dark at room temperature until an appropriate colour deposition was observed. Finally, the specimens were rinsed in distilled water (30°C, 30 min) to stop the colorimetric reaction. Cover slips were mounted using Aquatex (Merck, Darmstadt, Germany). The above methodology is based on the protocol described by Lambertsen et al. (Lambertsen et al., 2001).

ISH probes and validation

AP-labelled 28-mer cDNA probes were designed using the Oligo 6 software (Molecular Biology Insights, West Cascade, CO, USA) with standard settings (Table 2). Probes were designed in order to

Table 2. Sequences, probe and hybridisation information and references of AP-conjugated cDNA probes used for *in situ* hybridisation

Target mRNA	Probe sequence (5′-3′)	No. of bases	% GC	Base no. of cDNA	Hybridisation conditions		T_m (°C)	Reference
					SSC	% F		
α_{1a}	CCAAAGGCAAATGGGTTTAATATCATTG	28	35.7	3197-3224, inside cds.	4×	35	55.8	*O. mykiss*/AY319391
α_{1b}	GCAGCTGAGTGCACCATCACAGTGTTCA	28	53.6	3345-3372, inside cds.	4×	50	58.1	*O. mykiss*/AY319390
α_{1c}	CGGGGTAACACCTCAGAGAACTTGGTCC	28	57.1	3409-3436, inside cds.	4×	50	60.5	*O. mykiss*/AY319389
α_3	GACAGAAAGGGGGACCGGGGACGCCATG	28	67.9	3872-3900, outside cds.	1.5×	50	60.6	*O. mykiss*/AY319388
β-Actin	CCAGACTCGTCGTACTCCTGCTTGCTGA	28	57.1	1070-1097, inside cds.	4×	50	60.5	*S. salar*/AF012125

Probes were labelled with alkaline phosphatase at the 5′-terminus. cds, coding sequence; SSC, saline sodium citrate; % F, percent formamide; T_m, theoretical melting of DNA–RNA duplexes point using listed hybridisation conditions calculated according to Wilkinson, 1992 as $T_m = 79.8 + 18.5 \log$ (molarity of monovalent cations) + 0.58 (% GC content of probe) + 0.0012 (% GC)^2 – 0.5 (% formamide) – 820 / (probe length in bases).

Table 3. Sequences of 28-mer cDNAs used in competition experiments to validate *in situ* hybridisation probe specificity

Name	cDNA sequence (5′-3′)	Region in mRNA (base no.'s)	Identity with probe sequence	Reference (species/ acc. number)
α_{1b} sequence in α_{1a} probe region	ACAGTGTTCATTGGATGTAATGATAAGG	3328-3354	14/28	*O. mykiss*/AY319390
α_{1a} sequence in α_{1b} probe region	AGAGTTAGACACACAGTTACAGTAGCCA	1055-1082	14/28	*O. mykiss*/AY319391

The listed sequences were used in 10-fold excess in conjunction with the cross-matching isoform AP-conjugated *in situ* hybridisation (ISH) probe: i.e. α_{1b} sequence was combined with α_{1a} probe and *vice versa*.

have minimal hairpin and dimer formation, and all sequences were BLASTed. Due to the high similarity of the α-isoform sequences, each probe sequence was aligned against the other isoforms. Identity generally ranged between 10/28 and 16/28 bases.

Two series' of control hybridisation experiments were done in order to validate the specificity of the 28-mer cDNA probes. In one series, the specificity of the α_{1a} and α_{1b} probes were checked by co-incubating gill sections with the AP-conjugated cDNA probe (3 pmol ml^{-1}) for a particular target (α_{1a} *vs* α_{1b}) with 10-fold excess of the matching cDNA sequence of the alternate isoform in the probe region (see Table 3). In both cases, the identity between the AP-labelled probe and the cDNA sequence of the alternate isoform was 14/28. In another series, the ability of the unlabelled probe sequence to displace the AP-conjugated probe was checked by co-incubating tissue with the probe (3 pmol ml^{-1}) and 5-fold excess of the unlabelled cDNA sequence.

Statistics

All data was analyzed using two-way analysis of variance (ANOVA) followed by Bonferroni adjusted Fisher's Least Significant Difference (LSD) test, taking into account the total number of paired comparisons. When necessary, data was log-transformed to obtain normality and homogeneity of variances. In all cases, a significance level of $\alpha<0.05$ was used. All tests were performed using SAS (v. 9.1 for Windows, by SAS Institute, Cary, NC, USA).

RESULTS

Plasma sodium concentration (Fig. 1A) was elevated 12 h–3 days after SW transfer compared with corresponding FW groups. There was an overall effect of SW and a significant interaction between time and salinity. Gill Na^+,K^+–ATPase activity (Fig. 1B) varied insignificantly in the FW groups and was significantly elevated in the SW group at seven days post-transfer.

The α_{1a} transcript level was in the range 0.7–3.9 amol 20 ng^{-1} total RNA (Fig. 2A). α_{1a} Transcript levels were affected by both time and salinity and there was a significant interaction between the two factors, with SW-values being lower than FW-values at 3 and 7 days after transfer. The α_{1b} transcript level was in the range 0.5–5.3 amol 20 ng^{-1} total RNA (Fig. 2B). α_{1b} Transcript levels were affected by both time and salinity and there was a significant interaction between the two factors, with SW-values being higher than FW-values at 1, 3 and 7 days after transfer. The α_{1c} transcript level was in the range 0.3–0.4 amol 20 ng^{-1} total RNA (Fig. 2C). Overall, it was affected by time but not salinity and with a significant interaction between the two factors. The α_3 transcript level was in the range 0.02–0.05 amol 20 ng^{-1} total RNA (Fig. 2D) and was affected by salinity and time. The level was generally lower in SW than in FW. The sum of α-transcripts was in the range 3–7 amol 20 ng^{-1} total RNA (Fig. 2E) and was affected by both time and salinity with a significant interaction. The sum increased after SW-transfer being significantly higher at 3 and 7 days compared with the FW-level. The ratio of α_{1a}:α_{1b} was in the range 4–5 in FW and decreased to a lower value of 0.26 after SW-transfer (Fig. 2F). The ratio was significantly affected by both time and salinity and with a significant interaction.

The β_1 transcript level was in the range 0.07–0.3 amol 20 ng^{-1} total RNA (Fig. 3). β_1 Transcript levels were affected by time and salinity and there was a significant interaction between the two factors. The level was generally higher in SW than in FW, being significant at 12 h and 7 days.

The relative distributions of α-subunit isoforms in FW and after SW-transfer are shown in Fig. 4. In FW, the contribution of the four subunits was α_{1a}, 68–74%; α_{1b}, 15–23%; α_{1c}, 7–13%; α_3, 0.7–1.2%. After SW-transfer, a major shift in α_{1a} and α_{1b} was observed in favour of α_{1b} being the dominating isoform. Seven days post-transfer the relative proportions were: α_{1a}, 19%; α_{1b}, 75%. No major changes occurred in the relative contribution of α_{1c} and α_3, their shares being 4% and 1.7%, respectively, on day 7 in SW.

Localisation of α-subunits in the gill

The α_{1a} isoform was primarily located in cells in the interlamellar region at the base of the lamellae in both FW and SW gills (Fig. 5A,B). These cells were more numerous in FW than in SW

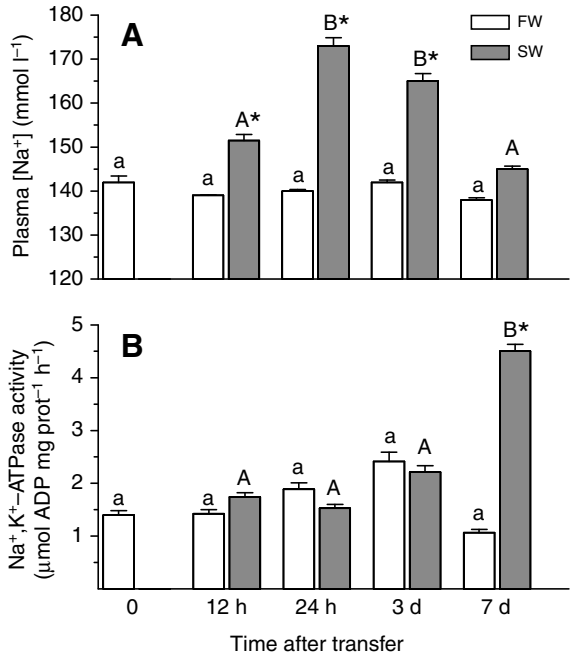

Fig. 1. The effect of FW–SW (closed bars) or FW–FW (open bars) transfers on plasma [Na^+] (A) and gill Na^+,K^+–ATPase activity (B) in Atlantic salmon. Different letters above bars indicate significant difference within FW (lowercase letters) or SW (uppercase letters). Asterisk indicates difference between FW and SW groups at a certain time point ($P<0.05$). FW, freshwater; SW, seawater.

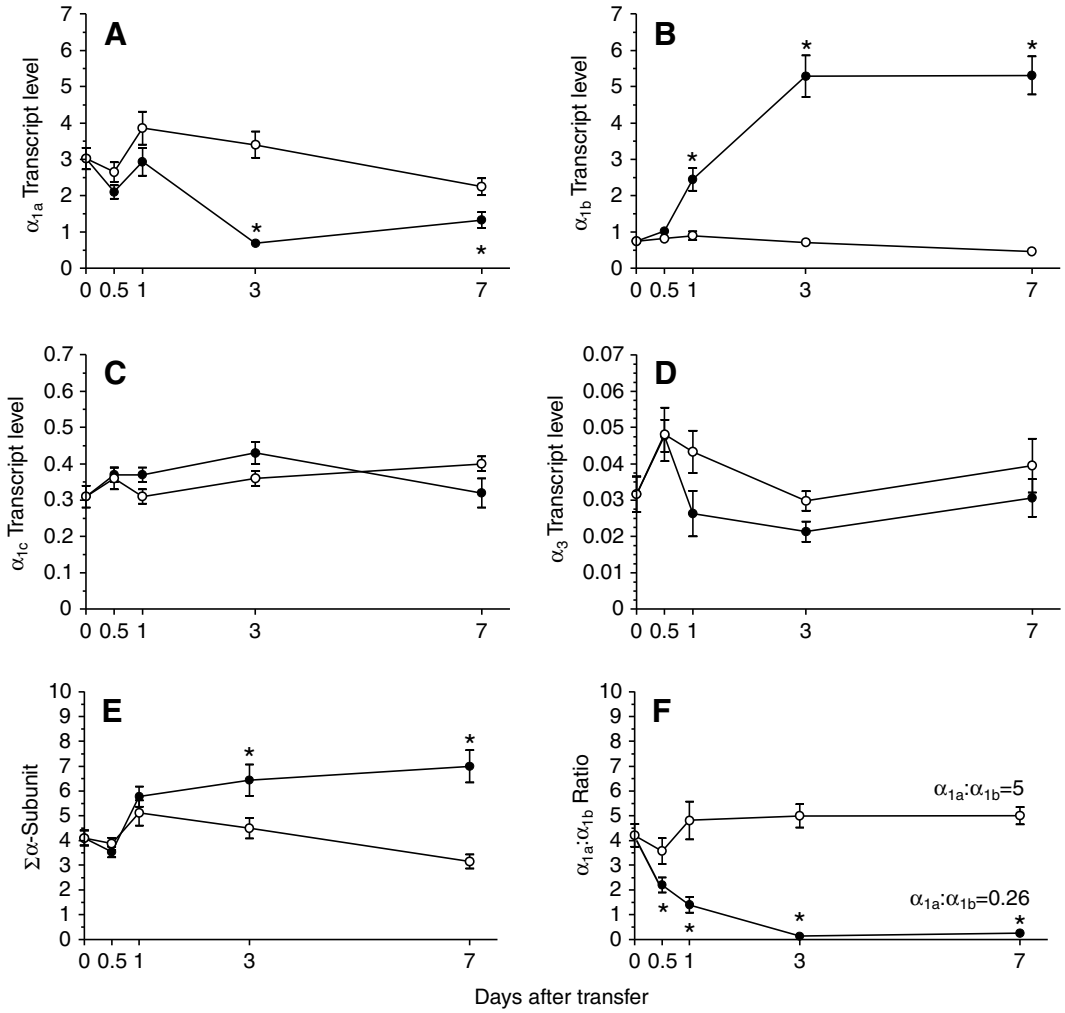

Fig. 2. The effect of FW–SW (closed symbols) or FW–FW (open symbols) transfers on α-subunit isoform mRNA levels (A, α_{1a}; B, α_{1b}; C, α_{1c}; D, α_3), the sum of α-subunit transcript levels (E) and the ratio between α_{1a} and α_{1b} in Atlantic salmon gill. Transcript levels are shown in amol 20 ng^{-1} total RNA. Asterisk indicate difference between FW and SW groups at a certain time point (P<0.05). FW, freshwater; SW, seawater.

gill sections (Fig. 5A–C *vs* Fig. 5D,E). Cells on the secondary lamellae also stained positive with the α_{1a} probe in FW (Fig. 5A-B) but this labelling disappeared in SW gills (Fig. 5D). The contour of the FW-cells was larger and they were often in contact with the surface of the epithelium (Fig. 5B) compared with SW-cells, which appeared smaller and deeper in the epithelium (Fig. 5D).

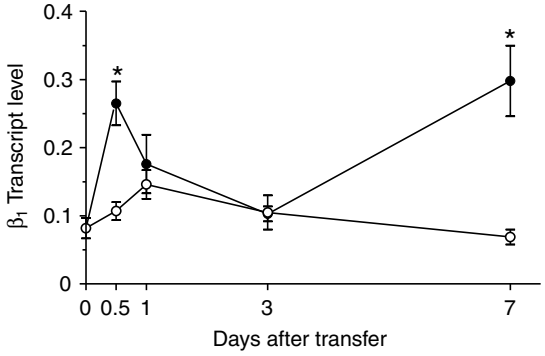

Fig. 3. The effect of FW–SW (closed symbols) or FW–FW (open symbols) transfers on β_1-subunit mRNA levels in Atlantic salmon gill. Transcript levels are shown in amol 20 ng^{-1} total RNA. Asterisk indicates the difference between FW and SW groups at a certain time point (P<0.05). FW, freshwater; SW, seawater.

In FW, the α_{1b} staining occurred in cells almost exclusively in the interlamellar region (Fig. 6A). The cells appeared small and deep in the epithelium, without contact with the apical surface of the epithelium. Rarely, labelling also appeared in cells on the lamellae. In SW-acclimated fish, there was a much higher density of positively reacting cells – again primarily in the interlamellar region of the filament epithelium (Fig. 6B-D). These cells were larger than those observed in FW and generally were in contact with the apical surface. In SW, there was no labelling of cells on the lamellae (Fig. 6B,C). Application of the α_{1c} or the α_3 probe gave no clear staining of gill cells either in FW or SW (not shown). The use of the β-actin probe gave a strong and almost uniform staining of all cell types in the gill (Fig. 6E).

Simultaneous incubation of gill sections with a specific cDNA probe (α_{1a} or α_{1b}) and the corresponding unlabelled cDNA sequence of the alternate isoform (α_{1b} or α_{1a}) in 10-fold excess, gave no changes in staining pattern or staining intensity as shown in Fig. 7A–D. Thus, the probes were highly isoform specific. However, simultaneous incubation of gill sections with a specific cDNA probe

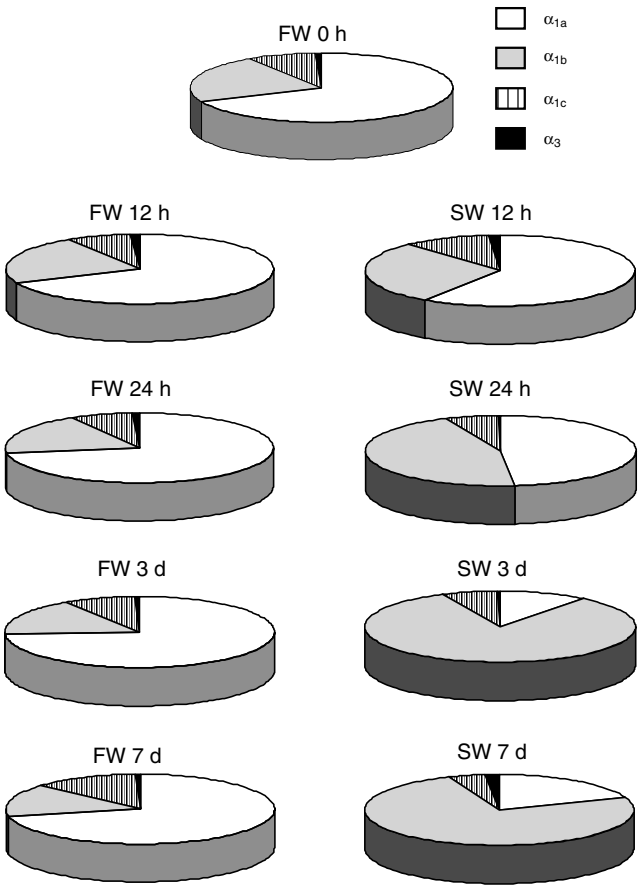

Fig. 4. Diagrams showing the relative distribution in gill tissue of the four analysed α-subunit isoforms during acclimation from FW–SW or during sham-transfer from FW–FW. The four isoforms are indicated by different degree of shading (α_{1a}, open; α_{1b}, grey; α_{1c}, hatched; α_3, black). FW, freshwater; SW, seawater.

(α_{1a} or α_{1b}) and the corresponding unlabelled cDNA sequence of the same isoform in 5-fold excess, completely displaced the hybridisation signal (Fig. 7E,F) (shown for α_{1b} only), showing that the hybridisation signal is target specific.

Quantitative considerations of α-subunit mRNA in chloride cells

Based on the present quantitative estimates of α-subunit mRNA in whole gill RNA extracts and a few simple assumptions, we can make a rough calculation of the fraction of the mRNA pool in chloride cells made up of α-subunit isoforms. Consider the following situation: the mRNA pool of gill tissue makes up 1–3% of the total RNA extract, thus in 20 ng of total RNA (1 QPCR reaction) the mRNA amounts to 0.2–0.6 ng. Assuming 100% efficiency in the first strand cDNA synthesis reaction this is all converted 1:1 into cDNA. The sum of α-subunit isoform transcript is presently found to be around 5 amol 20 ng^{-1} total RNA. The mean transcript size (of α_{1a} and α_{1b} isoforms) is 3350 bases (based on full length sequences in *O. mykiss*). With an approximate nucleotide molar weight of 307 g mol^{-1}, the mean molar weight of α-subunit mRNA is 1×10^6 g mol^{-1}. Thus, the mean weight of 5 amol α transcript is 5.2 pg. This amount equals 0.8–2.5% of the estimated mRNA pool in the gill extract. From the ISH analyses, α_{1a} and α_{1b} isoforms are predominantly located in presumed chloride cells in the gill. The relative fraction of mitochondrion-rich chloride cells have been estimated to be in the order of <10% of the total cell number in the gill (Goss et al., 2004). Assuming the mRNA content per cell is the same – irrespective of cell type – it can be estimated that the amount of α-subunit mRNA within the chloride cells makes up 8–25% of the total mRNA pool. Even though connected with some uncertainty, this gives a rough estimate of the total abundance of α-subunit transcripts in the chloride cells.

DISCUSSION

This is the first attempt to localise the α-isoforms of Na^+,K^+–ATPase in the gill of any fish species and to quantify all α- and β-isoforms in absolute terms at the mRNA level in response to a salinity change. Two α-subunit isoforms (α_{1a} and α_{1b}) were predominant in the gill irrespective of salinity and were present in almost equimolar amounts. They both varied in response to salinity whereas the additional α_{1c} and α_3 isoforms were expressed at lower levels – especially the α_3 isoform, which was present at negligible levels and showed little variation. Based on these measures, the sum of α-subunit transcripts is in the range of 5 amol α-subunit transcript per 20 ng total gill RNA, which we estimated to correspond to 8–25% of the mRNA pool within chloride cells. Even though some uncertainty is connected with this estimate, this is a very high fraction of total mRNA but matches well with the high abundance of Na^+,K^+–ATPase pumps estimated to reach 200 million pumps per chloride cell (Karnaky, 1980).

The α_{1a} and α_{1b} transcripts

The primers we used to quantify these two major transcripts were designed in order to obtain maximum isoform specificity. The α_{1b} primer pair was the same as used by Richards et al. (Richards et al., 2003) in *O. mykiss*, by Bystrianski et al. (Bystrianski et al., 2006; Bystrianski et al., 2007) in *S. alpinus* and *S. salar*, and by Shrimpton et al. (Shrimpton et al., 2005) in *O. nerka*. These primers were designed near the 3′-terminus, where there is a region of maximum heterology between the α-isoforms. In all of the above studies, however, the α_{1a}-primers were designed in the middle of the transcript in a region with very high identity between the isoforms. These primers had only one (forward) and two (reverse) mismatches compared with the α_{1b} sequence, and when tested against specific cDNA sequences of the two isoforms, they annealed and amplified the two isoforms with almost equal efficiency (not shown). Thus, in the former studies there is a risk that the α_{1a} primers may have amplified both α_{1a} and α_{1b} transcript. In order to avoid this, we designed the α_{1a}-primers in the 3′-region in order to obtain maximum isoform specificity (zero and 10 mismatches in forward and reverse primers, respectively) and when tested against the synthetic polynucleotide sequences of the two isoforms, they amplified only the α_{1a} isoform, as expected.

Our present study confirms previous reports of a reciprocal change of the two major α-isoforms in response to salinity change. When the salinity was increased from FW to SW, α_{1a} decreased and α_{1b} increased within a 1–3 day time course, the sum of these two showing a doubling. This pattern is in accordance with Richards et al. [(Richards et al., 2003) *O. mykiss*], Mackie et al. [(Mackie et al., 2005) *S. salar*] and Bystrianski et al. [Bystrianski et al., 2006) *S. alpinus*], who speculated that this pattern of regulation may reflect major functional differences of these isoforms with respect to their putative roles in ion uptake (α_{1a}) and ion secretion (α_{1b}), respectively. In maturing *O. nerka*, Shrimpton et al. (Shrimpton et al., 2005) found upregulation of α_{1a} upon FW entry; however, α_{1b} was unchanged after FW-encounter and upregulated in fish on the

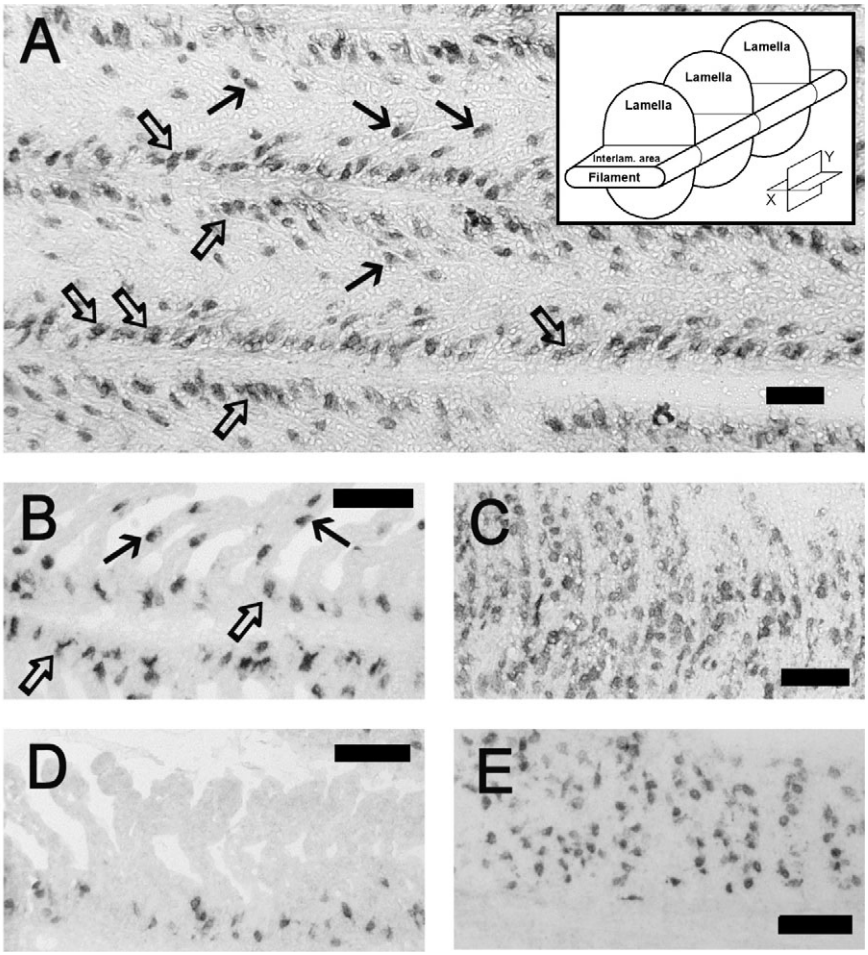

Fig. 5. Representative gill sections probed with the α_{1a} isoform AP-labelled cDNA probe. The insert in panel A shows orientation of sections: X-plane – frontal section; Y-plane – sagittal section. (A–C) Gills from FW salmon; (D,E) gills from SW salmon. A,B,D are sagittal sections, showing lamellae emerging perpendicularly from the filament. C,D are frontal sections at the base of the lamellae, showing cells in the interlamellar region. Solid arrows show labelled cells on lamellae, open arrows show labelled cells in filament. Gill sections were 10 μm thick. Bars indicate 100 μm. AP, alkaline phosphatase; FW, freshwater; SW, seawater.

spawning grounds, suggesting a non-specific response to stress in moribund fish.

There were already marked changes in the transcript levels on day 1 increasing until day 3 after SW-transfer. This is probably initiated by the osmotic stress apparent at 12 h and peaking on day 1, and mediated by osmoregulatory hormones, of which cortisol is a likely candidate (McCormick, 2001). Remarkably, Na^+,K^+–ATPase hydrolytic activity, which is a measure of total protein abundance, was not elevated until day 7. An overall increase in Na^+,K^+–ATPase activity is seen in response to hyperosmotic conditions in many euryhaline fish (Marshall, 2002), and a lag period of several days is not unusual (Bystrianski et al., 2006; Madsen et al., 1995). It has been argued that this reflects the time for protein synthesis in poikilothermic fish (Conte and Lin, 1967), however, we propose that *de novo* synthesis of 'secretory'-type Na^+,K^+–ATPase may be accomplished prior to that. Because the enzymatic assay does not separate between 'FW-absorptive-type' and 'SW-secretory-type' enzyme in the gill, the gross capacity is merely a static measure of a highly dynamic enzymatic pool reflecting the difference between protein being degraded and synthesised. Thus, new 'SW-secretory-type' (α_{1b}) Na^+,K^+–ATPase may be synthesised well before day 7 without being observed in measures of catalytic capacity, which also explains why plasma $[Na^+]$ is stabilised and already regulated after <3 days. The presence and reciprocal regulation of two dominating isoforms may be specific to salmonids, as in killifish, the α_{1a} isoform increases in both hyper- and hyposaline environments compared with brackish water (Scott et al., 2004) whereas the α_{1b} isoform remains unchanged.

The α_{1c} transcript

The α_{1c} variant of the α_1 isoform has only been described in salmonids [*O. mykiss* (Richards et al., 2003); *S. salar* (Nilsen et al., 2007)]. In the present study as well as the quoted studies, the transcript level of α_{1c} was unresponsive to salinity as well as during smoltification. The level was somewhat lower than the α_{1a} and α_{1b} isoforms. In *O. mykiss*, there is a universal tissue distribution of the transcript of this isoform (Richards et al., 2003) and if this also applies to cell types within the gill, this may lead to a very low transcript level per cell and thus explain why the isoform was not detected using AP-conjugated ISH probes. All together, the data conform with the 'house-keeping' function suggested by Richards et al. and Nilsen et al. (Richards et al., 2003; Nilsen et al., 2007).

The α_3 transcript

The levels of α_3 mRNA have only been reported in a single study in *O. mykiss*, where it was found to be unresponsive to SW (80% SW) (Richards et al., 2003) and is, thus, suggested to be a housekeeping isoform. In our present study, α_3 mRNA levels were extremely low in whole-gill extracts, making up only approximately 1% of the total α-transcript level. Despite this low level, α_3 showed an overall significant decrease in response to SW. Even if the transcript may be concentrated in a few specific cell types, the level is still very low. At the protein level, three studies have investigated

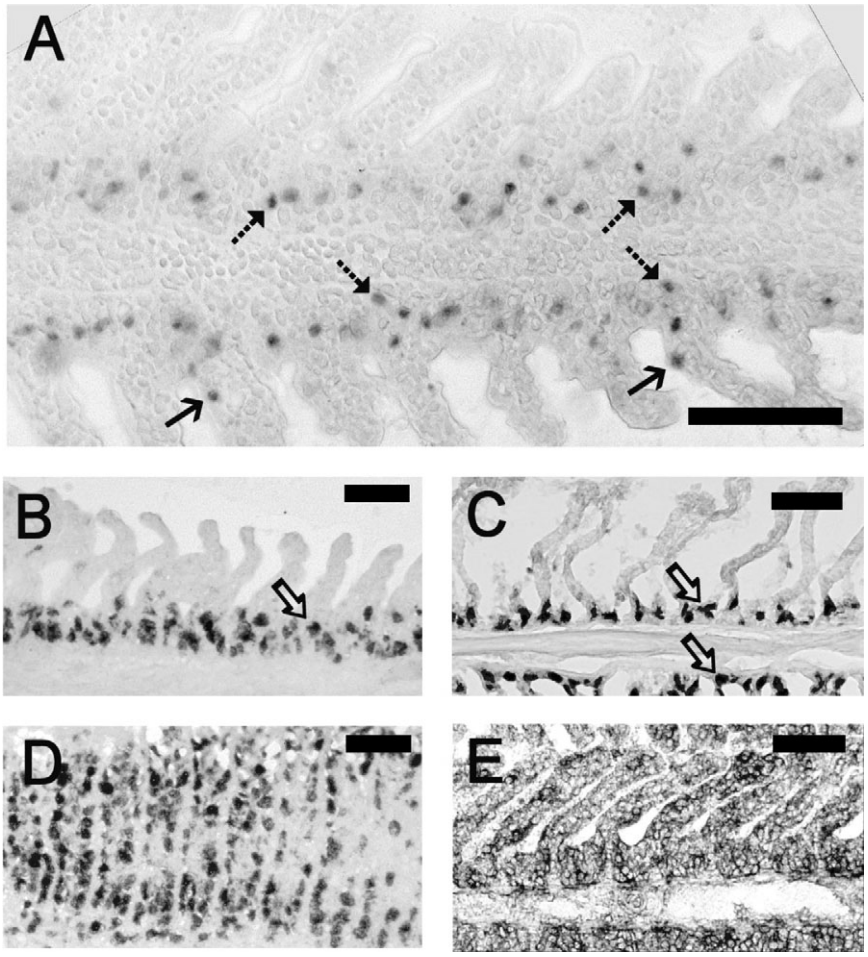

Fig. 6. Representative gill sections probed with the α_{1b} isoform with AP-labelled cDNA probe. (A) Gill from FW salmon; (B–D) gills from SW salmon; (E) gill section probed with β-actin cDNA probe. For orientation of sections refer to Fig. 5.A,B,C,E are sagital sections, showing lamellae emerging perpendicularly from the filament. D is a frontal section at the base of the lamellae, showing cells in the interlamellar region. Solid arrows show labelled cells on lamellae, broken arrows show labelled cells deep in the filament, open arrows show large labelled cells in filament with apical contact. Gill sections were 10 μm thick. Bars indicate 100 μm. AP, alkaline phosphatase; FW, freshwater; SW, seawater.

the presence of a α_3-like isoform in the gills of teleosts. Pressley reported lack of presence in the catfish gill by using a heterologous antibody (TED) raised against the rat α_3 isoform (Pressley, 1992). D'Cotta et al. detected the α_3 in *S. salar* gills using the same antibody (D'Cotta et al., 2000). The isoform was found in both FW parr and in FW and SW smolt but no attempts were made to quantify the abundance. The α_3 isoform was also reported in a study of euryhaline tilapia (Lee et al., 1998) (use of a polyclonal antibody against rat α_3), where it was found not to change in the gills after transfer to SW. This was in contrast to the α_1 in their study (use of polyclonal antibody against avian α_1), which was higher in gills of SW than FW fish. Both the α_1 and α_3 were localised by immunocytochemistry in MRC apparently belonging to different populations. Unfortunately, we were unable to localise the α_3 transcript in the salmon gill. We suspect that this is due to the extremely low abundance of the mRNA in this species.

The β_1 transcript

Whereas the α-subunit is the catalytic component determining the transport kinetics of the Na^+,K^+-ATPase, the β-subunit is essential for stabilisation of the α-subunit, membrane targeting, structural and functional maturation of the pump (Ackerman and Geering, 1990; Geering, 1990; Scheiner-Bobis, 2002). Compared with the α-subunit, very few studies have addressed the expression and regulation of the β-subunit in teleosts [*Danio rerio* (Appel et al., 1996); *Anguilla anguilla* (Cutler et al., 2000); *Sparus sarba* (Deane and Woo, 2005); *S. salar* (Nilsen et al., 2007)]. In mammals, three isoforms (β_1–β_3) are expressed in different tissues and may assemble with different α-isoforms, thus increasing the number of possible α, β-heterodimers considerably. In the eel, the β_1 and a duplicate β_1 isoform, named β_{233} are the only isoforms expressed in the gill (Cutler et al., 1995; Cutler et al., 2000) whereas a β_3 isoform is found exclusively expressed in the brain (Cutler et al., 1997). Both the β_1 and the β_{233} isoform showed a strong response to salinity changes in the eel gill and the latter also in other ion-transporting epithelia. We found that the β_1 transcript overall increased (doubled) after transfer to hypersaline conditions, with an initial peak at 24 h followed by an increase on day 7 after transfer. Remarkably, the absolute level of β_1 is considerably lower (approximately 1/50) than the sum of α-subunits, and assuming that the transcripts are localised in the same cell types, this suggests that the rate of β-subunit production may be a limiting step in generation of new pumps. β-Isoform multiplicity is unknown in salmonids at this moment but based on the present findings, it should be pursued in future studies. In mammalian and cellular model systems, there are examples of co-expression and regulation of the two subunits in both equimolar and different levels (Ewart and Klip, 1995). In these situations, where different transcript levels are found, the β-subunit transcript is usually expressed at the lower level (Young and Lingrell, 1987). In addition to differentially regulated rates of transcription, there is evidence that the translational efficiency of the β-subunit may be several-fold higher than the α-subunit, which may account for equal accumulation of the two subunit proteins in those cells and

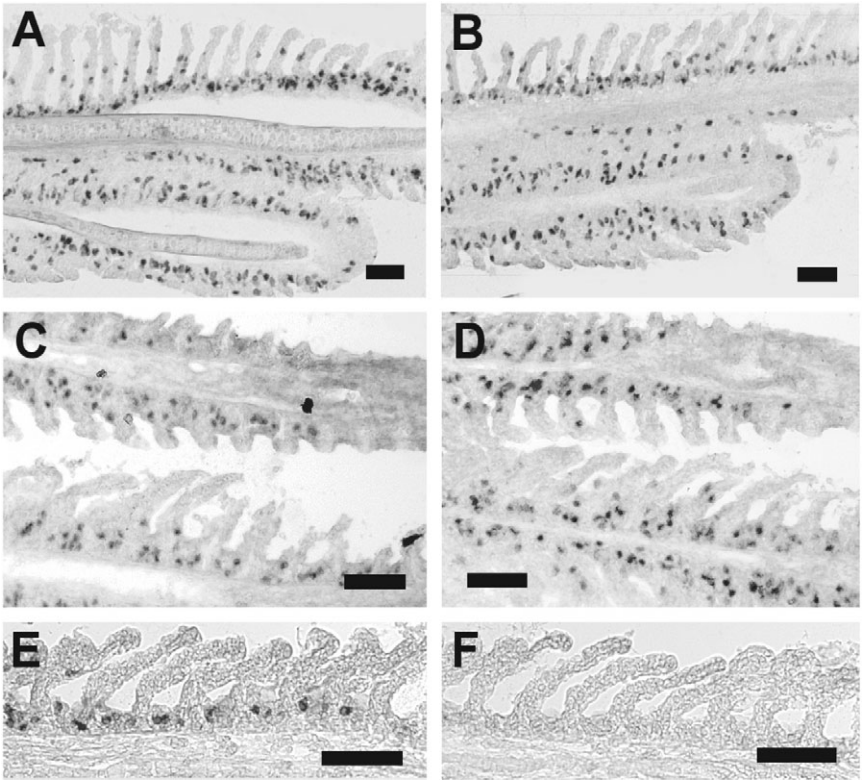

Fig. 7. Validation of probe specificity. Pair wise, adjacent FW gill sections were probed with AP-labelled α_{1a} (A,B) or α_{1b} (C,D) cDNA probes either alone (A,C) or in combination with 10-fold excess of the corresponding unlabelled cDNA sequence of the alternate isoform (i.e. α_{1b} in B and α_{1a} in D). No significant displacement of labelled probe takes place in either experiment, showing that the two probes are specific for their respective mRNA targets. (E,F) The sections were probed with the AP-labelled α_{1b} probe either alone, E, or in combination with 5-fold excess of the corresponding unlabelled α_{1b} cDNA sequence, F. The labelled probe was fully displaced under these conditions. Bars indicate 100 μm. AP, alkaline phosphatase; FW, freshwater.

tissues where α-mRNA is more abundant than β-mRNA. There are several examples of differential control of α- and β-subunit genes in cell systems (Corthésy-Theulaz et al., 1991; Farman et al., 1992; Geering et al., 1989) and one remarkable example among teleosts. Deane and Woo cloned both the α- and β-subunit in *S. sarba* gill and examined the response to various hormones (Deane and Woo, 2005). The two subunits were mostly regulated in parallel, even though absolute quantification was not performed. However, there was a remarkable divergence with regard to the effect of cortisol, which stimulated the α-subunit but had no effect on the β-subunit, neither at the mRNA nor the protein level. In agreement herewith, the authors found no effect of cortisol on Na^+,K^+–ATPase enzymatic activity. This clearly demonstrates that expression of the β-subunit in some instances may exert important control with overall pump abundance. Future studies should include analyses of α- as well as β-subunit expression to increase our understanding of their regulatory diversity.

Localisation of Na^+,K^+–ATPase α-isoforms in the gill

The mRNAs of the two predominant α_{1a} and α_{1b} isoforms were localised by ISH in the gill of *S. salar* whereas we were unsuccessful in localising the α_{1c} and α_3 isoforms. Based on the quantitative expression data, the obvious reason for the lack of success with the latter isoforms is their low level of expression in the gill. This is particularly the case for the α_3 isoform. Isoforms α_{1a} and α_{1b} were generally localised in discrete cells primarily in the filament epithelium but occasionally also in lamellar positions. Both isoforms were present in cells in FW and SW; however, their cellular expression pattern changed in a characteristic way, in accordance with the reciprocal regulation described above. Judged from their location, these cells correspond to mitochondrion-rich chloride cells of one type or another (see Introduction).

In FW, the α_{1a} isoform was localised in numerous cells in the interlamellar space and also frequently in cells on the lamellae. Most of these cells appeared elongated and large and were typically in contact with the apical (water) surface of the epithelium. The α_{1b} isoform was also expressed in cells in the interlamellar region but less so than the α_{1a} isoform. Occasionally, cells in the lamellae also stained positive for α_{1b}. However, in FW the α_{1b}-probe stained rounded cells, notably small and localised deep in the epithelium without contact with the apical surface. This suggests these cells to be non-functional, possibly immature differentiated chloride cells awaiting stimulus to become functionally mature. This stimulus for development appears to be under the influence of salinity, as the staining intensity and apparent many-fold increase in cell size in the SW-gill, the mRNA now being localised in large, elongated cells with apical contact exclusively in the interlamellar region. It seems probable that these cells represent the functional stage of the smaller cells described for the FW-gill – thus representing the secretory SW-type chloride cell. Not much is known about cellular differentiation mechanisms and morphogenesis of the various types of MRCs in the fish gill. However, a model of epidermal stem cell differentiation into various types of MRCs in zebrafish (*Danio rerio*) embryos has recently been proposed by Hsiao et al. (Hsiao et al., 2007).

In the SW gill, the α_{1a} mRNA is present in several cells – mostly in the interlamellar region and only rarely on the lamellae. These cells appear deeper in the epithelium than their FW-counterparts and may be non-functional. The general picture emerging from the localisation part of this study is in good agreement with the quantification data and shows a very morphoplastic gill epithelium with at least two cell types responsible for ion-transport being recruited to- and from- the epithelial surface in response to salinity. The mRNAs of α_{1a} and α_{1b} are present in the functional state as well as presumed precursor state of these cells, characterised by

their deeper position below the epithelial surface. This picture supports the hypothesis by Richards et al. that the α_{1a} isoform is predominantly involved in ion-uptake and α_{1b} is the isoform driving ion-secretion, even though both isoforms are present in the basolateral membrane network and pump Na^+ into the basolateral space (Richards et al., 2003). Whereas the localisation data suggest that expression of the α_{1b} isoform is exclusive to secretory-type chloride cells and their early differentiated stages, it cannot be excluded that the α_{1a} may also play a role in secretory-type chloride cells. This question shall await co-localisation studies with other proteins involved in ion secretion (e.g. CFTR, $Na^+K^+2Cl^-$ cotransporter) or ion absorption (e.g. ENaC, V-type H^+ATPase) respectively.

Perspectives

Successful acclimation to hypo- and hyperosmotic media requires a net reversal of ion transport across the gill epithelium. The recent, discovery of multiple Na^+,K^+–ATPase α-isoforms is an important step in understanding the molecular basis for this reversal (Richards et al., 2003). Our present study is the first to localise these isoforms in gill tissue, to investigate their dynamics during remodelling of the gill and to establish the real quantitative relationship between the transcript levels of the α-isoforms and the auxiliary β-subunit of Na^+,K^+–ATPase. Importantly, the histological evidence suggests that α_{1b} may be good marker for SW-type chloride cells and their putative precursor cells deeper in the filament whereas it cannot be excluded that α_{1a} may play a dual role in both FW- and SW-type chloride cells. The observed α_{1a}–α_{1b} isoform switch during FW–SW acclimation may form the molecular basis for the reversal of Na^+ transport across the gill epithelium (Jorgensen, 2008). In the SW gill, Na^+,K^+–ATPase may be rooted in glycosphingolipid-enriched rafts whereas the dominant isoform in FW (α_{1a}) due to sequence differences probably is not associated with rafts and it has been suggested that this leads to uncoupled Na^+ transport (Lingwood et al., 2005). A lysine substitution found in α_{1a} in the ion binding site may reduce the Na^+:ATP ratio from 3 to 2 making ion extrusion in FW thermodynamically more favourable (Jorgensen, 2008). In addition, a substitution of glutamate953 with serine in the α_{1a} isoform may interfere with interaction with FXYD peptides and thereby alter the affinities for Na^+ or K^+. With the recent findings that several FXYD isoforms are expressed in the salmon gill (Tipsmark, 2008), this may have important implications for the tuning of ion transport during osmotic adjustments. However, two interesting questions are open for future research: are the two main types of MRCs interconvertible and do they differentiate from the same stem cells given the right stimuli? There is elegant evidence that, at least in some species, both transformations may occur (Hiroi et al., 1999; Hsiao et al., 2007; Hwang and Lee, 2007).

LIST OF ABBREVIATIONS

AP	alkaline phosphatase
Ct	threshold cycle
FW	freshwater
ISH	*in situ* hybridisation
MRC	mitochondrion-rich cell
PCR	polymerase chain reaction
QPCR	quantitative polymerase chain reaction
SEI	sucrose–EDTA–imidazol
SW	seawater

The research was supported by a grant from The Danish Natural Research Council (272-06-0526) and a Postdoctoral Fellowship grant to C.K.T. from The Carlsberg Foundation (2005-1-311), and a grant from the School of Aquatic Sciences (SOAS, Denmark) to P.K.

REFERENCES

Ackermann, U. and Geering, K. (1990). Mutual dependence of Na,K–ATPase α- and β-subunits for correct posttranslational processing and intracellular transport. *FEBS Lett.* **269**, 105-108.

Appel, C., Gloor, S., Schmalzing, G., Schachner, M. and Bernhardt, R. R. (1996). Expression of a Na,K–ATPase β3 subunit during development of the Zebrafish central nervous system. *J. Neurosci. Res.* **46**, 551-564.

Augood, S. J., McGowan, E. M., Finsen, B. R., Heppleman, B. and Emson, P. C. (1993). Non-radioactive ISH using alkaline phosphatase-labeled oligonucleotides. In *In situ Hybridization: Biological Techniques Series* (ed. W. Wisden and B. J. Morris), pp. 81-97. New York: Academic Press.

Bystrianski, J. S., Richards, J. G., Schulte, P. M. and Ballantyne, J. S. (2006). Reciprocal expression of gill Na^+/K^+–ATPase α-subunit isoforms α1a and α1b during seawater acclimation of three salmonid fishes that vary in their salinity tolerance. *J. Exp. Biol.* **209**, 1848-1858.

Bystriansky, J. S., Frick, N. T., Richards, J. G., Schulte, P. M. and Ballantyne, J. S. (2007). Wild arctic char (*Salvelinus alpinus*) upregulate gill Na^+,K^+–ATPase during freshwater migration. *Physiol. Biochem. Zool.* **80**, 270-282.

Conte, F. P. and Lin, D. H. Y. (1967). Kinetics of cellular morphogenesis in gill epithelium during sea water adaptation of *Oncorhynchus* (Walbaum). *Comp. Biochem. Physiol.* **23**, 945-957.

Corthésy-Theulaz, I., Mérillat, A. M., Honegger, P. and Rossier, B. C. (1991). Differential regulation of Na-K-ATPase isoform gene expression by T_3 during rat brain development. *Am. J. Physiol. Cell Physiol.* **261**, C124-C131.

Cutler, C. P., Sanders, I. L., Hazon, N. and Cramb, G. (1995). Primary sequence, tissue specificity and mRNA expression of the Na^+,K^+–ATPase β1 subunit in the European eel (*Anguilla anguilla*). *Fish Physiol. Biochem.* **14**, 423-429.

Cutler, C. P., Sanders, I. L. and Cramb, G. (1997). Expression of Na^+,K^+–ATPase β subunit isoforms in the European eel (*Anguilla anguilla*). *Fish Physiol. Biochem.* **17**, 371-376.

Cutler, C. P., Brezillon, S., Bekir, S., Sanders, I. L., Hazon, N. and Cramb, G. (2000). Expression of a duplicate Na,K–ATPase β_1-isoform in the European eel (*Anguilla anguilla*). *Am. J. Physiol. Regul. Integr. Comp. Physiol.* **279**, R222-R229.

D'Cotta, H., Valotaire, C., Le Gac, F. and Prunet, P. (2000). Synthesis of gill Na^+,K^+–ATPase in Atlantic salmon smolts: differences in α-mRNA and α-protein. *Am. J. Physiol. Regul. Integr. Comp. Physiol.* **278**, R101-R110.

Deane, E. E. and Woo, N. Y. S. (2005). Cloning and characterization of sea bream Na^+-K^+–ATPase α and β subunit genes: *in vitro* effects of hormones on transcriptional and translational expression. *Biochem. Biophys. Res. Comm.* **1331**, 1229-1238.

Evans, D. H. (2008). Teleost fish osmoregulation: what have we learned since August Krogh, Homer Smith, and Ancel Keys? *Am. J. Physiol. Regul Integr. Comp. Physiol.* **295**, R704-R713.

Evans, D. H., Piermarini, P. M. and Choe, K. P. (2005). The multifunctional fish gill: dominant site of gas exchange, osmoregulation, acid–base regulation, and excretion of nitrogenous waste. *Physiol. Rev.* **85**, 97-177.

Ewart, H. S. and Klip, A. (1995). Hormonal regulation of the Na^+-K^+-ATPase: mechanisms underlying rapid and sustained changes in pump activity. *Am. J. Physiol. Cell Physiol.* **269**, C295-C311.

Farman, N., Coutry, N., Logvinenko, N., Blot-Chabaud, M., Bourbouze, R. and Bonvalet, J. P. (1992). Adrenalectomy reduces α_1 and not β_1 Na^+-K^+–ATPase mRNA expression in rat distal nephron. *Am. J. Physiol. Cell Physiol.* **263**, C810-C817.

Geering, K. (1990). Subunit assembly and functional maturation of Na,K–ATPase. *J. Membr. Biol.* **115**, 109-121.

Geering, K., Theulaz, I., Verrey, F., Häuptle, M. T. and Rossier, B. C. (1989). A role for the β-subunit in the expression of functional Na^+-K^+–ATPase in *Xenopus* oocytes. *Am. J. Physiol. Cell Physiol.* **257**, C851-C858.

Goss, G. G., Adamia, S. and Galvez, F. (2001). Peanut lectin binds to a subpopulation of mitochondria-rich cells in the rainbow trout gill epithelium. *Am. J. Physiol. Regul. Integr. Comp. Physiol.* **281**, R1718-R1725.

Guynn, S. R., Scofield, M. A. and Petzel, D. H. (2002). Identification of mRNA and protein expression of the Na/K–ATPase α1-, α2- and α3-subunit isoforms in Antarctic and New Zealand notothenid fishes. *J. Exp. Mar. Biol. Ecol.* **273**, 15-32.

Hiroi, J., Kaneko, T. and Tanaka, M. (1999). *In vivo* sequential changes in chloride cell morphology in the yolk-sac membrane of Mozambique tilapia (*Oreochromis mossambicus*) embryos and larvae during seawater adaptation. *J. Exp. Biol.* **202**, 3485-3495.

Hsiao, C. D., You, M. S., Guh, Y. J., Ma, M., Jiang, Y. J. and Hwang, P. P. (2007). A positive regulatory loop between *foxi3a* and *foxi3b* is essential for specification and differentiation of zebrafish epidermal ionocytes. *PLos ONE* **2**, e302.

Hwang, P. P. and Lee, T. H. (2007). New insights into fish ion regulation and mitochondrion-rich cells. *Comp. Biochem. Physiol.* **148A**, 479-497.

Jorgensen, P. L. (2008). Importance for absorption of Na^+ from freshwater of lysine, valine and serine substitutions in the α-1a-isoform of Na,K–ATPase in the gills of rainbow trout (*Oncorhynchus mykiss*) and Atlantic salmon (*Salmo salar*). *J. Membr. Biol.* **223**, 37-47.

Karnaky, K. J., Jr (1980). Ion-secreting epithelia: chloride cells in the head region of *Fundulus heteroclitus*. *Am. J. Physiol. Regul. Integr. Comp. Physiol.* **238**, R185-R198.

Keys, A. and Willmer, E. N. (1932). 'Chloride secreting cells' in the gills of fishes, with special reference to the common eel. *J. Physiol. (Lond.)* **76**, 368-378.

Lambertsen, K. L., Gregersen, R., Drøjdahl, N., Owens, T. and Finsen, B. (2001). A specific and sensitive method for visualization of tumor necrosis factor in the murine central nervous system. *Brain Res. Brain Res. Protoc.* **7**, 175-191.

Lee, T., Tsai, J., Fang, M., Yu, M. and Hwang, P. P. (1998). Isoform expression of the Na^+,K^+–ATPase α-subunit in gills of the teleost *Oreochromis mossambicus*. *Am. J. Physiol. Regul. Integr. Comp. Physiol.* **275**, R926-R932.

Lingwood, D., Harauz, G. and Ballantyne, J. S. (2005). Regulation of fish gill Na^+,K^+–ATPase by selective sulfatide-enriched raft partitioning during seawater adaptation. *J. Biol. Chem.* **280**, 36545-36550.

Mackie, P., Wright, P. A., Glebe, B. D. and Ballantyne, J. S. (2005). Osmoregulation and gene expression of Na^+/K^+–ATPase in families of Atlantic salmon (*Salmo salar*) smolts. *Can. J. Fish. Aquat. Sci.* **62**, 2661-2672.

Madsen, S. S., Jensen, M. K., Nohr, J. and Kristiansen, K. (1995). Expression of Na^+,K^+–ATPase in the brown trout *Salmo trutta*: *in vivo* modulation by hormones and seawater. *Am. J. Physiol. Regul. Integr. Comp. Physiol.* **269**, R1339-R1345.

Marshall, W. S. (2002). Na^+, Cl^-, Ca^{2+} and Zn^{2+} transport by fish gills: retrospective review and prospective synthesis. *J. Exp. Zool.* **293**, 264-283.

McCormick, S. D. (1993). Methods for nonlethal gill biopsy and measurements of Na^+,K^+–ATPase activity. *Can. J. Fish. Aquat. Sci.* **50**, 656-658.

McCormick, S. D. (2001). Endocrine control of osmoregulation in teleost fish. *Am. Zool.* **41**, 781-794.

Nilsen, T. O., Ebbesson, L. O. E., Madsen, S. S., McCormick, S. D., Andersson, E., Björnsson, B. T., Prunet, P. and Stefansson, S. O. (2007). Differential expression of gill Na^+,K^+-ATPase α- and β-subunits, $Na^+,K^+,2Cl^-$-cotransporter and CFTR anion channel in juvenile anadromous and landlocked strains of Atlantic salmon (*Salmo salar*). *J. Exp. Biol.* **210**, 2885-2896.

Pressley, T. A. (1992). Phylogenetic conservation of isoform-specific regions within α-subunit of Na^+,K^+-ATPase. *Am. J. Physiol.* **262**, C743-C751.

Rajarao, S. J., Canfield, V. A., Mohideen, M. A., Yan, Y. L., Postlethait, J. H., Cheng, K. C. and Levenson, R. (2001). The repertoire of Na,K–ATPase α and β subunit genes in the zebrafish, *Danio rerio*. *Genome Res.* **11**, 1211-1220.

Richards, J. G., Semple, J. W., Bystriansky, J. S. and Schulte, P. M. (2003). Na^+/K^+–ATPase α-isoform switching in gills of rainbow trout (*Oncorhynchus mykiss*) during salinity transfer. *J. Exp. Biol.* **206**, 4475-4486.

Rozen, S. and Skaletsky, H. (2000). Primer3 on the WWW for general users and for biologist programmers. *Methods Mol. Biol.* **132**, 365-386.

Scheiner-Bobis, G. (2000). The sodium pump. Its molecular properties and mechanics of ion transport. *Eur. J. Biochem.* **269**, 2424-2433.

Scott, G. R., Richards, J. G., Forbush, B., Isenring, P. and Schulte, P. M. (2004). Changes in gene expression in gills of the euryhaline killifish *Fundulus heteroclitus* after abrupt salinity transfer. *Am. J. Physiol. Cell Physiol.* **287**, C300-C309.

Seidelin, M., Madsen, S. S., Blenstrup, H. and Tipsmark, C. K. (2000). Time-course changes in the expression of Na^+,K^+–ATPase in gills and pyloric caeca of brown trout (*Salmo trutta*) during acclimation to seawater. *Phys. Biochem. Zool.* **73**, 446-453.

Shrimpton, J. M., Patterson, D. A., Richards, J. G., Cooke, S. J., Schulte, P. M., Hinch, S. G. and Farrell, A. P. (2005). Ionoregulatory changes in different populations of maturing sockeye salmon *Oncorhynchus nerka* during ocean and river migration. *J. Exp. Biol.* **208**, 4069-4078.

Tecott, L. H., Eberwine, J. H., Barchas, J. D. and Valentino, K. L. (1987). Methodological considerations in the utilization of *in situ* hybridization. In *In Situ Hybridization: Applications to Neurobiology* (ed. K. L. Valentino, J. H. Erberwine and J. D. Barchas), pp. 3-24. Oxford: Oxford University Press.

Tipsmark, C. K. (2008). Identification of FXYD protein genes in a teleost: tissue-specific expression and response to salinity change. *Am. J. Physiol. Regul. Integr Comp. Physiol.* **294**, R1367-R1378.

Tipsmark, C. K., Luckenbach, J. A., Madsen, S. S. and Borski, R. J. (2007). Insulin-like growth factor I (IGF-I) and branchial IGF receptor expression and localization during salinity acclimation in striped bass. *Am. J. Physiol. Regul. Integr. Comp. Physiol.* **292**, R535-R543.

Uchida, K., Kaneko, T., Yamauchi, K. and Hirano, T. (1996). Morphometrical analysis of chloride cell activity in the gill filaments and lamellae and changes in Na^+K^+ ATPase activity during seawater adaptation in chum salmon fry. *J. Exp. Zool.* **276**, 193-200.

Varsamos, S., Diaz, J. P., Charmantier, G., Flik, G., Blasco, C. and Connes, R. (2002). Branchial chloride cells in sea bass (*Dicentrarchus labrax*) adapted to fresh water, seawater, and doubly concentrated seawater. *J. Exp. Zool.* **293**, 12-26.

Wilkinson, D. G. (1992). The theory and practice of *in situ* hybridization. In *In Situ Hybridization, A Practical Approach* (ed. D. G. Wilkinson), pp. 1-13. Oxford: Oxford University Press.

Young, R. M. and Lingrel, J. B. (1987). Tissue distribution of messenger-RNAs encoding the alpha-isoforms and the beta-subunit of rat Na^+,K^+–ATPase. *Biochem. Biophys. Res. Commun.* **145**, 52-58.